Journal of chemical & engineering data

Article

pubs.acs.org/jced

Density, Electrical Conductivity, and Dynamic Viscosity of *N*-Alkyl-4-methylpyridinium Bis(trifluoromethylsulfonyl)imide

Qing-Shan Liu,[†,‡,§] Pei-Pei Li,[§] Urs Welz-Biermann,[§] Xiao-Xia Liu,*[,†] and Jian Chen*[,‡]

[†]Department of Chemistry, Northeastern University, Shenyang 110819, China

[‡]Lab of Advanced Rechargeable Batteries, Dalian Institute of Chemical Physics, Chinese Academy of Sciences, Dalian 116023, China

[§]China Ionic Liquid Laboratory, Dalian Institute of Chemical Physics, Chinese Academy of Sciences, Dalian 116023, China

Supporting Information

ABSTRACT: Two air and water stable hydrophobic ionic liquids *N*-alkyl-4-methylpyridinium bis(trifluoromethylsulfonyl)imide ($[C_n4mpy][NTf_2]$, n = 2, 4) were synthesized and characterized. The density, electrical conductivity, and dynamic viscosity were measured and estimated in the range of T = (278.15 to 363.15) K. The melting temperature, glass transition temperature, and decomposition temperature of the two ILs were determined according to the differential scanning calorimetry (DSC) and thermogravimetric analyzer (TG). The molecular volume, standard molar entropy, and lattice energy were estimated in terms of empirical equations on the basis of the density values. The electrical conductivity and dynamic viscosity values dependence on temperature were fitted by the Vogel−Fulcher−Tamman equation. The molar conductivity was calculated by the density and electrical conductivity.

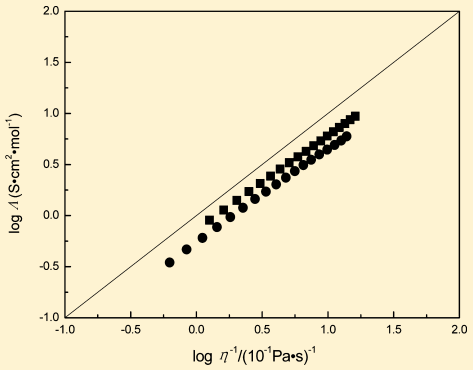

INTRODUCTION

In general, ionic liquids (ILs) exhibit outstanding physicochemical properties, such as low melting temperature, good solvation, negligible vapor pressure, high electrical conductivity, and thermal stability, which make them attractive in some particular applications. ILs have received more and more attention as valid potential green substitutes of many volatile organic solvents.[1−4]

Actually, most ILs are hydrophilic, so the hydrophobic ILs have attracted much more attention from the bis(trifluoromethylsulfonyl)imide $[NTf_2]^-$ as an anion in some fields.[5−8] This type of ILs exhibits a very wide liquid range, high electrical conductivity, and excellent thermal stability. However, the study of the mentioned ILs mainly focuses on the imidazolium cation.[9−12] Only a few researched the pyridinium cation-based ILs, and most studies were devoted to the density and dynamic viscosity.[13−16] The systematical research on the properties including density, dynamic viscosity, electrical conductivity, and so forth, are still scarce which can provide the good information of the suitable IL for a specific purpose.

Recently, the basic physicochemical properties of a series of ILs $[C_npy][NTf_2]$ (n = 2, 3, 4, 5, 6) have been reported by our group.[17−19] The basic physicochemical properties, including melting temperature, glass transition temperature, decomposition temperature, density, surface tension, electrical conductivity, and dynamic viscosity, were measured by the traditional methods. The other physicochemical properties, including molecular volume, standard molar entropy, lattice energy, parachor, molar enthalpy of vaporization, interstice volume, interstice fraction, and thermal expansion coefficient and activation energy, were estimated in terms of empirical and semiempirical equations on the basis of the experimental values.

In this study, the density, dynamic viscosity, and electrical conductivity of the ILs $[C_n4mpy][NTf_2]$ (n = 2, 4) were measured at different temperatures. The basic physicochemical properties were discussed. The effects of the alkyl chain length of the cation on density, electrical conductivity, and dynamic viscosity, respectively, were probed.

EXPERIMENTAL SECTION

Preparation of $[C_n4mpy][Br]$ and $[C_n4mpy][NTf_2]$ (n = 2, 4). $[C_n4mpy][Br]$ (n = 2, 4) was synthesized according to our previously reported method.[20] The final product was characterized by ^{1}H NMR spectra shown in Figures A and B of the Supporting Information. NMR analysis did not report any impurities. The ILs $[C_n4mpy][NTf_2]$ (n = 2, 4) were synthesized according to procedures from the literature.[17,18] The structures were identified by ^{1}H NMR and ^{13}C NMR (see Figures C, D, E, and F of the Supporting Information), and no impurities were found. The $AgNO_3/HNO_3$ solution was used to test the residual Br^- and the content below the detection limit of approximately 50 ppm. The final purity of the ILs was estimated better than 99 % in mass. The reaction equations are indicated as follows:

Received: May 27, 2012
Accepted: October 18, 2012
Published: October 31, 2012

Table 1. Values of Density, ρ/g·cm^{-3}, Dynamic Viscosity, η/mPa·s, Electrical Conductivity, σ/mS·cm^{-1}, and Molar Electrical Conductivity, Λ/S·cm^2·mol^{-1}, of ILs [C$_2$4mpy][NTf$_2$] and [C$_4$4mpy][NTf$_2$] at Pressure p = 0.1 MPa[a]

	ρ/g·cm^{-3}		η/mPa·s		σ/mS·cm^{-1}		Λ/S·cm^2·mol^{-1}	
T/K	[C$_2$4mpy] [NTf$_2$]	[C$_4$4mpy] [NTf$_2$]	[C$_2$4mpy] [NTf$_2$]	[C$_4$4mpy] [NTf$_2$]	[C$_2$4mpy] [NTf$_2$]	[C$_4$4mpy] [NTf$_2$]	[C$_2$4mpy] [NTf$_2$]	[C$_4$4mpy] [NTf$_2$]
278.15	1.5100[b]	1.4373[b]	79.45[c]	159.65[c]	3.39[d]	1.24	0.90	0.35
283.15	1.5052	1.4328	61.98[c]	118.57[c]	4.24	1.66	1.13	0.47
288.15	1.5010	1.4284	49.30[c]	90.07[c]	5.25	2.15	1.41	0.61
293.15	1.4961	1.4234	39.89[c]	69.82[c]	6.38	2.73	1.72	0.77
298.15	1.4920	1.4187	32.75	55.14	7.63	3.41	2.06	0.97
303.15	1.4877	1.4140	27.31	44.20	9.01	4.19	2.44	1.19
308.15	1.4830	1.4093	23.10	35.85	10.50	5.09	2.85	1.45
313.15	1.4783	1.4047	19.69	29.61	12.08	6.00	3.29	1.72
318.15	1.4734	1.4002	16.95	24.77	13.78	7.02	3.76	2.02
323.15	1.4688	1.3958	14.66	20.85	15.54	8.17	4.26	2.35
328.15	1.4644	1.3913	12.85	17.86	17.50	9.41	4.81	2.72
333.15	1.4599	1.3869	11.34	15.37	19.55	10.75	5.39	3.12
338.15	1.4551	1.3825	10.10	13.42	21.7	12.07	6.00	3.51
343.15	1.4506[b]	1.3777[b]	9.07	11.65	23.9[d]	13.56[d]	6.62	3.96
348.15	1.4460[b]	1.3731[b]	8.19	10.15	26.2[d]	15.10[d]	7.28	4.42
353.15	1.4414[b]	1.3686[b]	7.43	8.89	28.5[d]	16.70[d]	7.95	4.91
358.15	1.4369[b]	1.3640[b]	6.76	7.94	31.0[d]	18.38[d]	8.67	5.42
363.15	1.4323[b]	1.3594[b]	6.19	7.20[c]	33.5[d]	20.11[d]	9.40	5.95

[a]The uncertainty is ± 0.0002 g·cm^{-3} for density. The uncertainties are ± 1 % for electrical conductivity, dynamic viscosity, and molar electrical conductivity. The uncertainty is ± 0.05 K for temperature. [b]Calculated from empirical eq 1. [c]Calculated from empirical eq 4. [d]Calculated from empirical eq 4.

dx.doi.org/10.1021/je3004645 | J. Chem. Eng. Data 2012, 57, 2999−3004

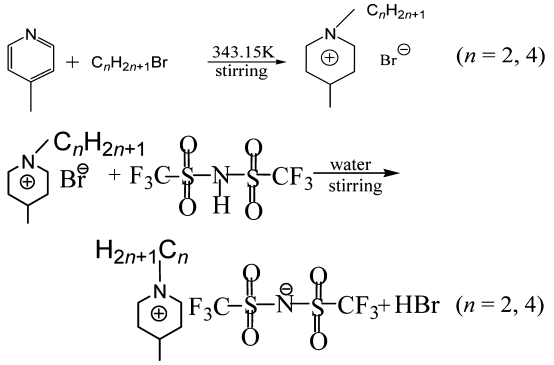

Thermodynamic Property. Differential scanning calorimetry (DSC) was carried out on NETZSCH DSC 204 at a heating rate of 10 K·min^{-1} under nitrogen atmosphere over a temperature window of (153 to 373) K. The temperature was directly cooled to 153 K by the liquid nitrogen. The decomposition temperature of the ILs was determined on a Netzsch TG 209 at a heating rate of 10 K·min^{-1} under the nitrogen atmosphere over a temperature range of (313 to 873) K (see Figures G, H, I, and J of the Supporting Information of DSC and TG).

Water Content. Although [C_n4mpy][NTf_2] (n = 2, 4) are hydrophobic ILs, water still exists in the ILs after drying by common methods. The presence of water becomes the most problematic impurity and needs to be confirmed before and after measurement. The water contents are less than 500 ppm before measurement and less than 800 ppm after measurement by a Cou-Lo Aquamax Karl Fischer moisture meter (v.10.06).

Density, Electrical Conductivity, and Dynamic Viscosity Measurements. The density, electrical conductivity, and dynamic viscosity of the samples were determined according to a previous paper[17−19,21] in the temperature range of T = (283.15 to 338.15) K for density, T = (298.15 to 363.15) K for dynamic viscosity, and T = (278.15 to 338.15) K for electrical conductivity, respectively. The values are listed in Table 1. The experimental error is ± 0.0002 g·cm^{-3} for density. The uncertainties are about ± 1 % for electrical conductivity and dynamic viscosity.

RESULTS AND DISCUSSION

Thermal Analysis. From Figures G and I of the Supporting Information, there are two endothermic peaks for [$C_2$4mpy][NTf_2], which indicated that it probably has the transition from solid to solid at 278.2 ± 0.1 K. There are two exothermic peaks for [$C_4$4mpy][NTf_2] at 235.8 ± 0.1 K and 242.2 ± 0.1 K, which indicated that it has two crystal forms. The glass transition temperatures and melting temperatures are listed in Table 2.

From Figures H and J of the Supporting Information, the samples exhibited the excellent thermal stability up to 630.0 K at the scanning rate of 10 K·min^{-1}. The mass loss of the two ILs is more than 90 % from the onset temperature to the terminal temperature. The mass losses of 5 %, 10 %, 20 %, 50 %, 80 %, and 90 % are listed in Table S1, which is shown in the Supporting Information.

Table 2. Molecular Weight and Thermal Properties from the DSC

	MW/g·mol^{-1}	T_m/K	T_g/K
[$C_2$4mpy][NTf_2]	402.32	291.0 ± 0.1	198.6 ± 0.1
[$C_4$4mpy][NTf_2]	430.38	292.4 ± 0.1	195.0 ± 0.1

Density. The density of this work is 1.4187 g·cm^{-3} for [$C_4$4mpy][NTf_2] at 298.15 K, which has a small discrepancy with the density value of 1.4122 g·cm^{-3} for [$C_4$4mpy][NTf_2].[15]

The temperature dependence on the density values in the range of the measurement can be fitted by the following equation:

$$\rho = A + BT \quad (1)$$

where ρ is the density; A and B are adjustable parameters. The fitting curves can be obtained (see Figure 1).The best fitting values and correlation coefficients are listed in Table 3.

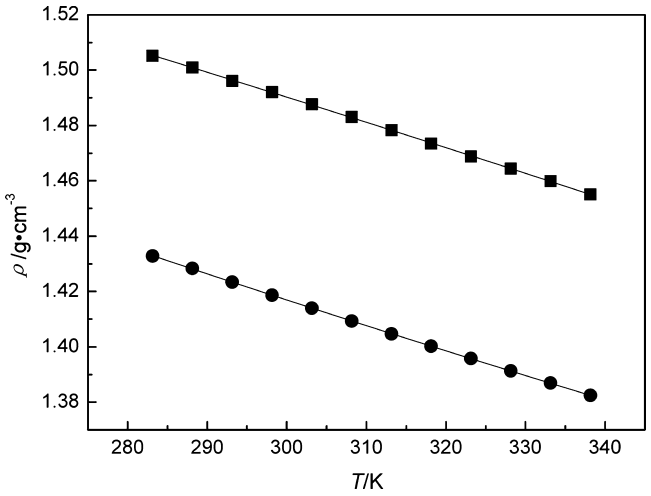

Figure 1. Plot of density, ρ, vs T/K. ■, [$C_2$4mpy][NTf_2]; ●, [$C_4$4mpy][NTf_2].

Table 3. Adjustable Parameters A and B, Correlation Coefficients (R), and Standard Deviations (s) for ILs [$C_2$4mpy][NTf_2] and [$C_4$4mpy][NTf_2], Derived from eq 1,

ILs	A	B	R	s
[$C_2$4mpy][NTf_2]	1.7642	−9.14·10^{-4}	0.99976	2.81·10^{-4}
[$C_4$4mpy][NTf_2]	1.6924	−9.17·10^{-4}	0.99971	3.37·10^{-4}

A straight line can be obtained by plotting ln ρ against T/K, and the empirical equation is:

$$\ln \rho/\text{g·cm}^{-3} = b - \alpha(T/\text{K}) \quad (2)$$

where b is an empirical constant, and the negative value of the slope, $\alpha = -(\partial \ln \rho/\partial T)_p$, is the thermal expansion coefficient of the sample. The fitting equations are ln ρ/g·cm^{-3} = 0.5840 − 6.17·10^{-4}(T/K), R = 0.99965 for [$C_2$4mpy][NTf_2] and ln ρ/g·cm^{-3} = 0.5441 − 6.52·10^{-4}(T/K), R = 0.99985 for [$C_4$4mpy][NTf_2]. The thermal expansion coefficients are 6.17·10^{-4} K^{-1} for [$C_2$4mpy][NTf_2] and 6.52·10^{-4} K^{-1} for [$C_4$4mpy][NTf_2], respectively. It increases with the increase of the alkyl chain length of the cation. The values are in good agreement with the range of 5·10^{-4} and 7·10^{-4} K^{-1} obtained by Jacquemin et al.[11]

The molecular volume, V_m, standard molar entropy, S^0, and lattice energy, U_{POT}, were calculated from experimental density using the empirical equations. The process of the calculation has been described in previous literature.[21] The obtained data from the empirical equations are listed in Table 4.

dx.doi.org/10.1021/je3004645 | J. Chem. Eng. Data 2012, 57, 2999−3004

Table 4. Estimated Values of Physicochemical Properties of $[C_2 4mpy][NTf_2]$ and $[C_4 4mpy][NTf_2]$ at 298.15 K

property	$[C_2 4mpy][NTf_2]$	$[C_2 4mpy][NTf_2]$
MW/g·mol^{-1}	402.33	430.38
V_m/nm^3	0.4479	0.5039
10^4 α/K^{-1}	6.17	6.52
V/cm^{-3}·mol^{-1}	269.7	303.4
S^0/J·K^{-1}·mol^{-1}	587.8	657.6
U_{pot}/kJ·mol^{-1}	410	399

From the Table 1 and Figure 1, the values of the density decrease with the increase of the alkyl chain length of the cation. From Table 4, the mean contribution of the methylene to the molecular volume is 0.0280 nm^3 of the samples $[C_n4mpy][NTf_2]$ (n = 2, 4) at 298.15 K. It is in good agreement with the values of 0.0280 nm^3 for ILs $[C_npy][NTf_2]$,[17] 0.0282 nm^3 for $[C_nmim][NTf_2]$,[22] and 0.0279 nm^3 for amino acid type ILs.[23−26]

Electrical Conductivity and Dynamic Viscosity. The dynamic viscosity is 55.14 mPa·s for $[C_4 4mpy][NTf_2]$ at 298.15 K, which is a little different from the dynamic viscosity of 56.300 mPa·s.[15]

The electrical conductivity and dynamic viscosity of the samples as a function of temperature are illustrated in Figures 2

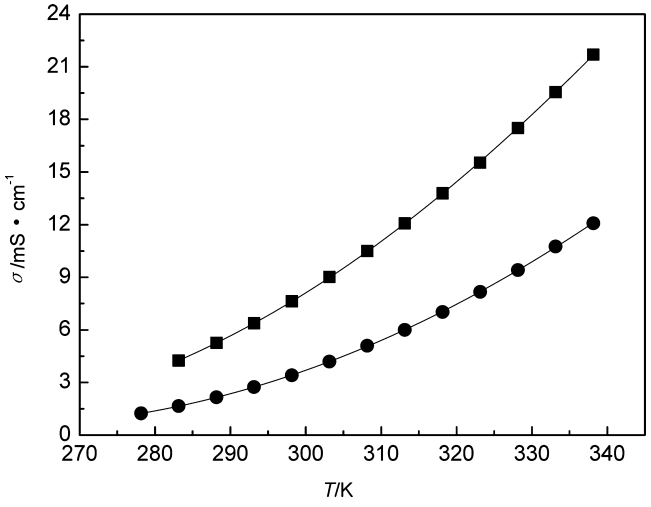

Figure 2. Plot of electrical conductivity, σ, vs T/K. ■, $[C_2 4mpy][NTf_2]$; ●, $[C_4 4mpy][NTf_2]$.

and 3. From the results, the dynamic viscosity decreases drastically with the increase of the temperature for each IL. However, the electrical conductivity behaves inversely. The dynamic viscosity increases with the extension of the alkyl side chain of the cation. However, the electrical conductivity greatly contrasts with the dynamic viscosity. The conclusion can be obtained that the electrical conductivity decreases with the dynamic viscosity increase for the samples.

The molar electrical conductivity can be obtained according to the following equation:

$$\Lambda = \sigma M \rho^{-1} \tag{3}$$

where Λ is the molar conductivity, σ is the electrical conductivity, M is the molar mass, and ρ is the density. The values of the molar conductivity are listed in Table 1.

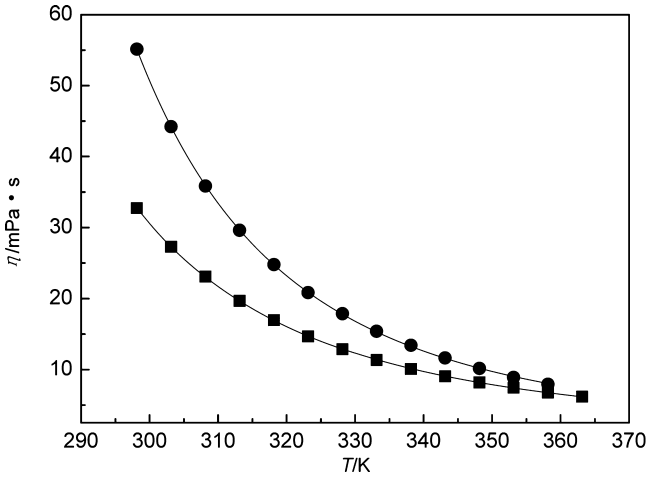

Figure 3. Plot of dynamic viscosity, η, vs T/K. ■, $[C_2 4mpy][NTf_2]$; ●, $[C_4 4mpy][NTf_2]$.

The temperature dependence of electrical conductivity, dynamic viscosity, and molar electrical conductivity values of the ILs can be fitted using the Vogel−Fulcher−Tamman (VFT) equation:

$$D = D_0 \exp(\pm B/(T - T_0)) \tag{4}$$

where D is the dynamic viscosity, electrical conductivity, or molar electrical conductivity; D_0 and B are adjustable parameters. The best fitted parameters of D_0, B, T_0, correlation coefficient, R, and standard deviation, s, are listed in Table 5. From Table 5, the obtained values of the correlation coefficient, R, are more than 0.9999, which indicates that the VFT equation can be used for fitting the experimental dynamic viscosity and electrical conductivity.

For electrical conductivity, the Arrhenius equation is:

$$\sigma = \sigma_\infty \exp(-E_\sigma/(k_B T)) \tag{5}$$

where E_a is the activation energy for electrical conduction, which indicates the energy needed for an ion to hop to a free hole, σ_∞ is the maximum electrical conductivity, and k_B is the Boltzmann constant. The $1000/T$ dependence on ln σ was plotted for ILs $[C_n4mpy][NTf_2]$ (n = 2, 4) (see Figure 4). From Figure 4, the curves are not straight lines (the red lines). So, the values of the experimental do not follow the Arrhenius behavior well by eq 5.

Cabeza et al.[27] have related the fitting parameters of the VFT equation with the Arrhenius equation: $D_0 = \sigma_\infty$ and $B = E_\sigma/k_B$, and the final version of the VFT equation is:

$$\sigma = \sigma_\infty \exp(-E_\sigma/(k_B(T - T_0)) \tag{6}$$

The activation energies of electrical conduction for ILs $[C_n4mpy][NTf_2]$ (n = 2, 4) were calculated and are listed in Table 5. From Table 5, the activation energies of electrical conductivity increases with the extension of the alkyl side chain.

For dynamic viscosity, the $1000/T$ dependence on ln σ was plotted for ILs $[C_n4mpy][NTf_2]$ (n = 2, 4) (see Figure 5) according to the Arrhenius equation. The Arrhenius equation is:

$$\eta = \eta_\infty \exp(E_\eta/(k_B T)) \tag{7}$$

where E_η is the activation energy for viscous flow, η_∞ is the maximum dynamic viscosity, and k_B is the Boltzmann constant. From Figure 5, the curves do also not form straight lines (the

dx.doi.org/10.1021/je3004645 | J. Chem. Eng. Data 2012, 57, 2999−3004

Table 5. Fitted Values of Dynamic Viscosity, Electrical Conductivity, and Molar Electrical Conductivity of η_0, σ_0, Λ_0, B, E_σ, E_η, T_0, Correlation Coefficients (R), and Standard Deviations (s)

		VFT equation					
property	IL	η_0/mPa·s	B/K	E_η/eV	T_0/K	R	s
η/mPa·s	[$C_2$4mpy][NTf_2]	0.1768	720.6	$62.2\cdot10^{-3}$	160.2	0.99997	0.043
	[$C_4$4mpy][NTf_2]	0.0859	914.6	$78.9\cdot10^{-3}$	156.6	0.99996	0.104
		σ_0/S·cm^{-1}	B/K	E_σ/eV	T_0/K	R	s
σ/mS·cm^{-1}	[$C_2$4mpy][NTf_2]	0.64	574.6	$49.6\cdot10^{-3}$	168.5	0.99997	$3.36\cdot10^{-2}$
	[$C_4$4mpy][NTf_2]	0.50	586.5	$50.6\cdot10^{-3}$	180.4	0.99996	$3.48\cdot10^{-2}$
		$10^{-2}\Lambda_0$/ S·cm^2·mol^{-1}		B/K	T_0/K	R	s
Λ/S·cm^2·mol^{-1}	[$C_2$4mpy][NTf_2]	2.12		619.0	164.7	0.99999	$1.61\cdot10^{-2}$
	[$C_4$4mpy][NTf_2]	1.78		635.6	176.2	0.99999	$0.80\cdot10^{-2}$

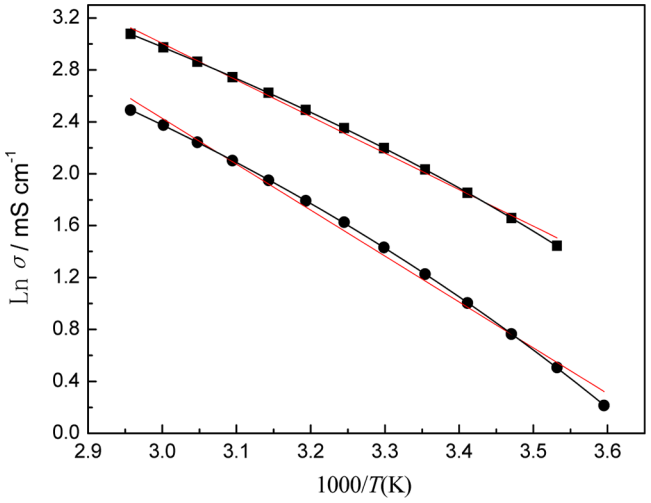

Figure 4. Plot of ln σ vs 1000/(T/K). ■, [$C_2$4mpy][NTf_2]; ●, [$C_4$4mpy][NTf_2]. The red line represents the linearized curve.

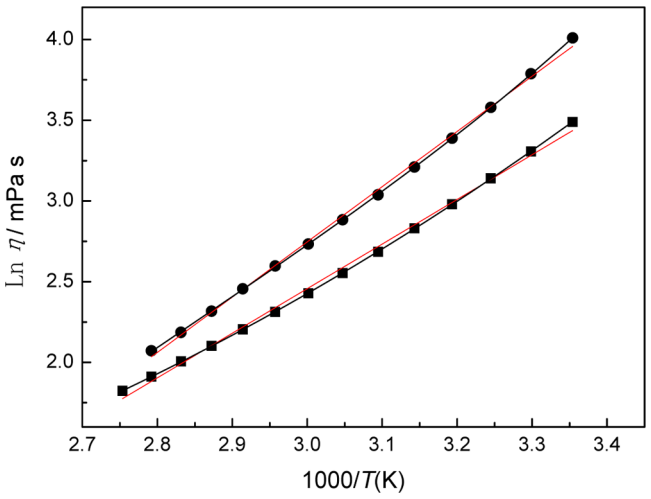

Figure 5. Plot of ln η vs 1000/(T/K). ■, [$C_2$4mpy][NTf_2]; ●, [$C_4$4mpy][NTf_2]. The red line represents the linearized curve.

red lines). So, the experimental values of the dynamic viscosity do not follow the Arrhenius behavior well by eq 7.

According to the Cabeza et al.[27] discussion, the VFT equation for dynamic viscosity was also related with the Arrhenius equation, and the final version of the VFT equation is:

$$\eta = \eta_\infty \exp(E_a/(k_B(T - T_0)) \quad (8)$$

The activation energies of dynamic viscosity for ILs [C_n4mpy][NTf_2] (n = 2, 4) were calculated and are listed in Table 5. From Table 5, the activation energies of dynamic viscosity increases with the extension of the alkyl side chain.

The Walden product can be used to describe the relationship of the molar conductivity and dynamic viscosity:

$$\Lambda\eta = k \quad (9)$$

where Λ is the molar conductivity, η is the dynamic viscosity, and k is a temperature-dependent constant. The Walden products (in [S·cm^2·mol^{-1}][cP]) are 67 for [$C_2$4mpy][NTf_2] and 53 for [$C_4$4mpy][NTf_2] at 298.15 K, respectively.

The log Λ dependence on log η^{-1} were plotted for ILs [C_n4mpy][NTf_2] (n = 2, 4) from (278.15 to 363.15) K (see Figure 6). From Figure 6, the curves approximate to straight

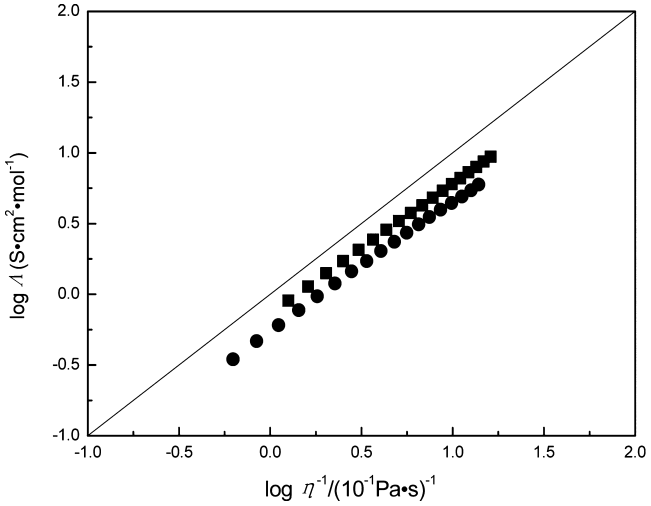

Figure 6. Walden plots for samples at temperatures from (278.15 to 353.15) K: ■, [$C_2$4mpy][NTf_2]; ●, [$C_4$4mpy][NTf_2]; the solid straight line is the ideal line for a 0.01 M aqueous KCl solution.

lines. The slopes of the lines for ILs [$C_2$4mpy][NTf_2] and [$C_4$4mpy][NTf_2] are 0.915 and 0.912, respectively. The position of the ideal line was established using aqueous KCl solutions at high dilution. The lines for ILs [C_n4mpy][NTf_2] (n = 2, 4) lie below and close to the ideal KCl line. The ILs [C_n4mpy][NTf_2] (n = 2, 4) are "subionic".[28]

CONCLUSIONS

The density, dynamic viscosity, and electrical conductivity of two air and water stable hydrophobic ILs [C_n4mpy][NTf_2] (n = 2, 4) were measured and estimated in the range of T =

dx.doi.org/10.1021/je3004645 | J. Chem. Eng. Data 2012, 57, 2999−3004

(278.15 to 363.15) K. The density and dynamic viscosity of the samples decrease with the increase in temperature; however, the conductivity behaves inversely. The dynamic viscosity increases with the extension of the alkyl side chain of the cation, while the density and electrical conductivity have an opposite trend. The molar volume increment per the addition of two carbon atoms, 33.7 $cm^3 \cdot mol^{-1}$, is obtained at 298.15 K. The melting temperatures of the two ILs are below 295 K. The samples exhibited excellent thermal stability up to 630 K. The VFT equation can be used to fit the dynamic viscosity and electrical conductivity of ILs. The ILs $[C_n4mpy][NTf_2]$ (n = 2, 4) are "subionic".

■ ASSOCIATED CONTENT

Supporting Information

NMR, DSC, and TG curves of $[C_n4mpy][NTf_2]$ (n = 2, 4) and table of mass loss of the two ILs. This material is available free of charge via the Internet at http://pubs.acs.org.

■ AUTHOR INFORMATION

Corresponding Author

*E-mail: xxliu@mail.neu.edu.cn (X.-X.L.). chenjian@dicp.ac.cn (J.C.).

Funding

This work was financially supported by the National Nature Science Foundation of China under Grant: NSFC No. 21203193, 50973013, and 21273029.

Notes

The authors declare no competing financial interest.

■ REFERENCES

(1) Rantwijk, F. V.; Sheldon, R. A. Biocatalysis in ionic liquids. *Chem. Rev.* **2007**, *107*, 2757−2785.

(2) Greaves, T. L.; Drummond, C. J. Protic Ionic Liquids: Properties and Applications. *Chem. Rev.* **2008**, *108*, 206−237.

(3) Hapiot, P.; Lagrost, C. Electrochemical Reactivity in Room-Temperature Ionic Liquids. *Chem. Rev.* **2008**, *108*, 2238−2264.

(4) Jessop, P. G.; Subramaniam, B. Gas-Expanded Liquids. *Chem. Rev.* **2007**, *107*, 2666−2694.

(5) Kim, G. T.; Appetecchi, G. B.; Alessandrini, F.; Passerini, S. Solvent-free, PYR_{1A}TFSI ionic liquid-based ternary polymer electrolyte systems I. Electrochemical characterization. *J. Power Sources* **2007**, *171*, 861−869.

(6) Orita, A.; Kamijima, K.; Yoshida, M.; Yang, L. Application of sulfonium-, and thioxonium-based salts as electric double-layer capacitor electrolytes. *J. Power Sources* **2010**, *195*, 6970−6976.

(7) Lazzari, M.; Mastragostino, M.; Pandolfo, A. G.; Ruiz, V.; Soavi, F. Role of Carbon Porosity and Ion Size in the Development of Ionic Liquid based Supercapacitors. *J. Electrochem. Soc.* **2011**, *158* (1), A22−A25.

(8) Orita, A.; Kamijima, K.; Yoshida, M. Allyl-functionalized ionic liquids as electrolytes for electric double-layer capacitors. *J. Power Sources* **2010**, *195*, 7471−7479.

(9) Rebelo, L. P. N.; Lopes, J. N. C.; Guedes, H. J. R.; Łachwa, J.; Najdanovic-Visak, V.; Visak, Z. P. Accounting for the unique, doubly dual nature of ionic liquids from a molecular thermodynamic and modeling standpoint. *Acc. Chem. Res.* **2007**, *40*, 1114−1121.

(10) Gardas, R. L.; Freire, M. G.; Carvalho, P. J.; Marrucho, I. M.; Fonseca, I. M. A.; Ferreira, A. G. M.; Coutinho, J. A. P. High-pressure densities and derived thermodynamic properties of imidaolium-based ionic liquids. *J. Chem. Eng. Data* **2007**, *52*, 80−88.

(11) Jacquemin, J.; Husson, P.; Padua, A. A. H.; Majer, V. Density and viscosity of several pure and water-saturated ionic liquids. *Green Chem.* **2006**, *8*, 172−180.

(12) Azevedo, R. G. D.; Esperança, J. M. S. S.; Szydlowski, J.; Visak, Z. P.; Pires, P. F.; Guedes, H. J. R.; Rebelo, L. P. N. Thermophysical and thermodynamic properties of ionic liquids over an extended pressure range: $[bmim][NTf_2]$ and $[hmim][NTf_2]$. *J. Chem. Thermodyn.* **2005**, *37*, 888−899.

(13) Crosthwaite, J. M.; Muldoon, M. J.; Dixon, J. K.; Anderson, J. L; Brennecke, J. F. Phase transition and decomposition temperatures, heat capacities and viscosity of pyridinium ionic liquids. *J. Chem. Thermodyn.* **2005**, *37*, 559−568.

(14) Gardas, R. L.; Costa, H. F.; Freire, M. G.; Carvalho, P. J.; Marrucho, I. M.; Fonseca, I. M. A.; Ferreira, A. G. M.; Coutinho, J. A. P. Densities and derived thermodynamic properties of imidazolium-, pyridinium-, pyrrolidinium-, and piperidinium-based ionic liquids. *J. Chem. Eng. Data* **2008**, *53*, 805−811.

(15) Oliveira, F. S.; Freire, M. G.; Carvalho, P. J.; Coutinho, J. A. P.; Lopes, J. N. C.; Rebelo, L. P. N.; Marrucho, I. M. Structural and positional isomerism influence in the physical properties of pyridinium NTf_2-based ionic liquids: pure and water-saturated mixtures. *J. Chem. Eng. Data* **2010**, *55*, 4514−4520.

(16) Yunus, N. M.; Mutalib, M. I. A.; Man, Z.; Bustam, M. A.; Murugesan, T. Thermophysical properties of 1-alkylpyridinium bis(trifluoromethylsulfonyl)imide ionic liquids. *J. Chem. Thermodyn.* **2010**, *42*, 491−495.

(17) Liu, Q. S.; Yang, M.; Yan, P. F.; Liu, X. M.; Tan, Z. C.; Welz-Biermann, U. Density and surface tension of ionic liquids $[C_npy][NTf_2]$ (n = 2, 4, 5). *J. Chem. Eng. Data* **2010**, *55*, 4928−4930.

(18) Liu, Q. S.; Yang, M.; Li, P. P.; Sun, S. S.; Welz-Biermann, U.; Tan, Z. C.; Zhang, Q. G. Physicochemical Properties of Ionic Liquids $[C_3py][NTf_2]$ and $[C_6py][NTf_2]$. *J. Chem. Eng. Data* **2011**, *56*, 4094−4101.

(19) Liu, Q. S.; Yan, P. F.; Yang, M.; Tan, Z. C.; Li, C. P.; Welz-Biermann, U. Dynamic viscosity and conductivity of ILs $[C_npy][NTf_2]$ (n = 2, 4, 5). *Acta Phys. Chim. Sin.* **2011**, *27* (12), 2762−2766.

(20) Tong, B.; Liu, Q. S.; Tan, Z. C.; Welz-Biermann, U. Thermochemistry of alkyl pyridinium bromide ionic liquids: Calorimetric measurements and calculations. *J. Phys. Chem. A* **2010**, *114*, 3782−3787.

(21) Liu, Q. S.; Tong, J.; Tan, Z. C.; Welz-Biermann, U.; Yang, J. Z. Density and surface tension of ionic liquid $[C_2mim][PF_3(CF_2CF_3)_3]$ and prediction of properties $[C_nmim][PF_3(CF_2CF_3)_3]$ (n = 1, 3, 4, 5, 6). *J. Chem. Eng. Data* **2010**, *55*, 2586−2589.

(22) Glasser, L. Lattice and phase transition thermodynamics of ionic liquids. *Thermochim. Acta* **2004**, *421*, 87−93.

(23) Fang, D. W.; Tong, J.; Guan, W.; Wang, H.; Yang, J. Z. Predicting properties of amino acid ionic liquid homologue of 1-alkyl-3-methylimidazolium glycine. *J. Phys. Chem. B* **2010**, *114*, 13808−13814.

(24) Fang, D. W.; Guan, W.; Tong, J.; Wang, Z. W.; Yang, J. Z. Study on physicochemical properties of ionic liquids based on alanine $[C_nmim][Ala]$ (n = 2, 3, 4, 5, 6). *J. Phys. Chem. B* **2008**, *112* (25), 7499−7505.

(25) Tong, J.; Song, B.; Wang, C. X.; Li, L.; Guan, W.; Fang, D. W.; Yang, J. Z. Prediction of the physicochemical properties of valine ionic liquids $[C_nmim][Val]$ (n = 2, 3, 4, 5, 6) by semiempirical methods. *Ind. Eng. Chem. Res.* **2011**, *50*, 2418−2423.

(26) Xu, W. G.; Ma, X. X.; Li, L.; Tong, J.; Guan, W. Prediction of the physicochemical properties of valine ionic liquids $[C_nmim][Val]$ (n = 2, 3, 4, 5, 6) by semiempirical methods: 2. *Ind. Eng. Chem. Res.* **2012**, *51*, 4105−4111.

(27) Vila, J.; Ginés, P.; Pico, J. M.; Franjo, C.; Jiménez, E.; Varela, L. M.; Cabeza, O. Temperature dependence of the electrical conductivity in EMIM-based ionic liquids. Evidence of Vogel-Tamman-Fulcher behavior. *Fluid Phase Equilib.* **2006**, *242*, 141−146.

(28) Belieres, J. P.; Angell, C. A. Protic ionic liquids: preparation, characterization, and proton free energy level representation. *J. Phys. Chem. B* **2007**, *111* (25), 4926−4937.